HHS Public Access

Author manuscript

Neuron. Author manuscript; available in PMC 2017 March 02.

Published in final edited form as:

Neuron. 2016 March 2; 89(5): 1059–1073. doi:10.1016/j.neuron.2016.01.023.

Cannabinoid control of learning and memory through HCN channels

Mattia Maroso[1,2], **Gergely G. Szabo**[1,2], **Hannah K. Kim**[1,2], **Allyson Alexander**[1], **Anh D. Bui**[1,2], **Sang-Hun Lee**[2,4], **Beat Lutz**[3], and **Ivan Soltesz**[1]

[1]Department of Neurosurgery, Stanford University, Stanford, CA, 94305, USA

[2]Department of Anatomy and Neurobiology, University of California, Irvine, CA 92697, USA

[3]Institute of Physiological Chemistry, University Medical Center of the Johannes Gutenberg University, Mainz 55128, Germany

Summary

The mechanisms underlying the effects of cannabinoids on cognitive processes are not understood. Here we show that cannabinoid type-1 receptors (CB1Rs) control hippocampal synaptic plasticity and spatial memory through the hyperpolarization-activated cyclic nucleotide-gated (HCN) channels that underlie the h-current (I_h), a key regulator of dendritic excitability. The CB1R-HCN pathway, involving c-Jun-N-terminal kinases (JNKs), nitric oxide synthase and intracellular cGMP, exerts a tonic enhancement of I_h selectively in pyramidal cells located in the superficial portion of the CA1 pyramidal cell layer, whereas it is absent from deep-layer cells. Activation of CB1R-HCN pathway impairs dendritic integration of excitatory inputs, long-term potentiation (LTP) and spatial memory formation. Strikingly, pharmacological inhibition of I_h or genetic deletion of HCN1 abolishes CB1R-induced deficits in LTP and memory. These results demonstrate that the CB1R-I_h pathway in the hippocampus is obligatory for the action of cannabinoids on LTP and spatial memory formation.

Introduction

Cannabinoid type-1 receptors (CB1Rs), upon activation by either endocannabinoids or exogenous agonists, potently inhibit neurotransmitter release, including GABA and glutamate (Katona et al., 1999; Mackie, 2005). Consistent with their modulation of neurotransmission, CB1Rs play a critical role in short- and long-term synaptic plasticity and memory formation (Castillo et al., 2012; Soltesz et al., 2015). For example, CB1R activation

Corresponding author: Mattia Maroso; Department of Neurosurgery, Stanford University, Stanford, CA, 94305, USA. mmaroso@stanford.edu.

[4]Present address: Department of Neurology, University of Arkansas for Medical Sciences, Little Rock, AR, 72205, USA

Author Contributions

M.M. and I.S. designed the experiments; M.M., G.G.S., A.A., A.B. and S.-H.L. performed in vitro experiments and analysis; H.K. performed in vivo behavioral analysis; M.M., B.L. and I.S. wrote the paper.

disrupts long-term potentiation (LTP) in the hippocampus (Zhu, 2006) and impairs spatial memory, whereas pharmacological inhibition of CB1Rs enhances spatial memory (Basavarajappa and Subbanna, 2014). However, in spite of the fact that several CB1R-mediated signaling pathways have been identified in both neuronal and non-neuronal cells (Metna-Laurent and Marsicano, 2015), the mechanisms by which CB1R activation interferes with LTP and spatial memory are not completely understood.

A major regulator of dendritic excitability and integration of synaptic inputs is the hyperpolarization-activated cationic depolarizing current (I_h), mediated by hyperpolarization-activated cyclic nucleotide-gated (HCN) channels which are predominantly expressed postsynaptically in the distal dendrites of hippocampal pyramidal cells (PCs) (He et al., 2014). Overall, I_h modulates dendritic excitability and learning and memory (Shah, 2014); for example, mice lacking HCN1 show enhanced LTP and hippocampal-dependent spatial memory (Nolan et al., 2004).

Based on the fact that activation of CB1Rs and HCNs has remarkably similar inhibitory effects on LTP and on spatial memory formation, we hypothesized the existence of a common mechanism by which CB1Rs and HCNs affect cognition. We used a combination of *in vitro* electrophysiological and *in vivo* behavioral experiments to demonstrate a novel signaling pathway where endogenous and exogenous activation of CB1Rs modulates I_h in a specific subset of CA1 PCs. Activation of this pathway decreases integration of excitatory synaptic inputs as well as LTP and limits spatial memory formation, whereas its inhibition enhances dendritic integration and LTP and prevents spatial memory impairments caused by exogenous cannabinoids.

RESULTS

Modulation of CB1Rs alters the depolarizing sag in superficial CA1 PCs

In order to determine whether cannabinoids affect spatial memory formation by modulating I_h, we first analyzed the effects of CB1R modulation on HCN-mediated, postsynaptic I_h in CA1 PCs in the dorsal hippocampus, a brain area involved in spatial memory formation. Specifically, we tested if CB1Rs modulate the hyperpolarization-induced depolarizing sag, a measure of postsynaptic I_h, using *in vitro* somatic whole cell recordings in current clamp configuration (Fig 1A). In order to isolate I_h from other postsynaptic membrane currents, these experiments were carried out in the presence of blockers of ion channels (voltage-gated K^+, Na^+, Ca^{2+}, inwardly rectifying K^+), and ionotropic and metabotropic neurotransmitter receptors (AMPA, NMDA, group I, II, and III metabotropic glutamate receptors (mGluRs), $GABA_A$ and $GABA_B$ receptors; see Experimental procedures). Note that inhibition of voltage-gated Na^+ and Ca^{2+} channels had the additional advantage of blocking presynaptic neurotransmitter release, therefore, CB1R-mediated presynaptic inhibition of neurotransmission could not underlie cannabinoid effects on postsynaptic I_h. As previously reported (Jarsky et al., 2008; Lee et al., 2014), sag amplitude was significantly greater in superficial PCs (SPCs), located close to the stratum radiatum, than in deep PCs (DPCs), located close to the stratum oriens (for definitions, see Lee et al., 2014). For example, at −100pA, the sag amplitude in SPCs was 4.2±0.2mV, compared to 2.5±0.1mV in

DPCs ($p<0.01$, Fig 1B,D; S1A; Tables S1,S2; for n values, see figure legends). Therefore, we analyzed the CB1R modulation of sag responses separately for SPCs and DPCs.

Bath application of WIN55,212 (WIN; 0.5μM), a synthetic CB1R agonist, significantly increased the sag response in SPCs by ~75% (Fig 1A,B; Table S1), providing the first indication that cannabinoids modulate I_h. This effect was specific to SPCs, because WIN had no effect on the smaller, but still measurable sag response in DPCs (Fig 1C,D; Table S2). We next investigated whether the WIN effect on sag amplitude in SPCs was mediated by CB1Rs. We tested the effect of WIN both in slices that had been pre-incubated in AM251, a specific CB1R antagonist (and inverse agonist; 10μM), and in slices obtained from mice lacking CB1R (CB1RKO). In both cases, there was no change in sag amplitude in SPCs after WIN application (Fig 1B; Table S1), supporting the idea that WIN acted through CB1Rs. In addition, sag amplitude at the baseline (i.e., before the application of WIN) in SPCs recorded from either AM251-treated slices or CB1RKOs was significantly reduced compared to their respective controls (Fig 1B; Table S1), suggesting that tonic CB1R activation enhanced the baseline level of I_h in SPCs. Conversely, AM251-treated and CB1RKO-derived DPCs showed similar sag amplitudes compared to their respective controls (Fig. 1D; Table S2). Furthermore, in the presence of AM251 or in CB1RKOs, the sag amplitude was similar in SPCs and DPCs (Fig 1B,D, S1A). Note that, in the experiments in SPCs, WIN and AM251 did not change the peak hyperpolarization induced by the current steps, therefore, the CB1R-dependent modulation of sag was not due to different I_h activation induced by different levels of membrane hyperpolarization (Table S6; see also below for voltage clamp experiments). In addition, the sag amplitude at baseline and the effect of WIN on sag in SPCs were similar between 3–4 week old (the age of mice in the experiments described above) and 8–10 week old animals (used in all experiments related to HCN1KOs and their respective controls; for rationale, see Supplemental Experimental Procedures; compare Fig 1B to Fig S1B and Table S1). In order to determine whether the CB1R modulation of sag amplitude occurred through HCNs, we tested the effect of pharmacological HCN inhibition (with ZD7288; 0.1mM) or genetic HCN1 deletion on sag amplitude both at baseline and after WIN application. Pharmacological inhibition or genetic deletion of HCN resulted in an almost complete abolishment of the sag response both in SPCs and DPCs, and subsequent WIN application did not increase the sag amplitude in either population (Fig 1B,D; Tables S1,S2). Taken together, these results strongly suggested that the CB1R-dependent sag modulation was mediated by HCN1-dependent I_h and that these effects were present in SPCs but not DPCs.

CB1Rs modulate somatic and distal dendritic I_h in SPCs

While the data above provided a strong initial indication of the existence of a functional CB1R to HCN pathway, it should be noted that the sag response is an indirect measure of postsynaptic I_h. Therefore, we next measured I_h using whole-cell voltage clamp recordings at the soma of CA1 SPCs in control conditions and in the presence of WIN. We compared the membrane potential for half-maximal I_h activation (V_{50}) before and after WIN application, and found that WIN significantly shifted the activation curve for I_h towards more depolarized values by 3.5mV in SPCs (Fig S2A; Table S3).

However, I_h and HCN channel density are greatest in the distal dendrites (Magee, 1998; Nusser, 2009). Therefore, we measured I_h using cell-attached voltage clamp recordings at distal dendrites (200–250μm from soma) in SPCs and DPCs before and after exogenous CB1R activation (with WIN) or inhibition (with AM251; Fig 2A–C,E; Table S3). We first compared V_{50} between SPCs and DPCs at baseline (i.e., before WIN), and found that the I_h activation curve in SPCs was shifted towards depolarized values in comparison to DPCs (Table S3; Fig S2B). In addition, WIN application significantly shifted V_{50} by 3.6 mV towards even more depolarized values in SPCs (Table S3; Fig 2A,B,E), without affecting V_{50} in DPCs (Table S3). In SPCs, the WIN-induced increase in I_h was significant even at low levels of hyperpolarization (e.g., amplitude of I_h: at −70mV: control, 13.2±0.9pA; WIN, 17.8±1.0pA; n=11–13; $p<0.05$), but WIN had no effect on maximal I_h amplitude (Table S4) or the k value of the Boltzmann fit of the activation curve (control, 9.1±0.4; WIN, 8.9±0.3; n=11–13; $p>0.05$).

Next, we repeated the previous experiments in the presence of AM251 and in CB1RKOs. After AM251 application, the V_{50} for I_h activation in SPCs was significantly shifted towards hyperpolarized values by 3mV, and a similar hyperpolarizing shift (2.7mV) was found in CB1RKOs (Table S3; Fig 2C,E–G). In addition, WIN did not change V_{50} in SPCs in CB1RKOs (Table S3; Fig 2F,G) and AM251 reversed the depolarizing shift in V_{50} induced by WIN (Table S3; Fig 2D,E; the maximal I_h amplitude did not change in any of the experimental conditions; Table S4). In contrast, the V_{50} measured in DPCs remained unchanged after AM251 application and in CB1RKOs (Table S3). Note that, in the presence of AM251 or in CB1RKOs, there was no difference in V_{50} values between SPCs and DPCs (Fig S2B; Table S3). Taken together, these whole-cell somatic and cell-attached distal dendritic voltage clamp recordings, in agreement with the current-clamp data, revealed the presence of a tonic CB1R-dependent elevation of I_h and a further potentiation of I_h by exogenous cannabinoids selectively in SPCs.

In addition, because I_h influences key intrinsic membrane properties, including input resistance (R_{in}) and resting membrane potential (V_m), we analyzed the effects of WIN, AM251 and their combination on R_{in} and V_m in SPCs. As expected from an increase in I_h, WIN significantly decreased R_{in} and induced a small but significant depolarization of V_m (Table S6). The effect was present both at the soma and at distal dendrites, with the latter site showing a stronger modulation. In contrast, AM251 or the co-application of WIN +AM251 increased R_{in} and induced a V_m hyperpolarization both at the soma and distal dendrites, with the latter showing stronger modulation (Table S6). These results are consistent with the ability of CB1Rs to modulate I_h in SPCs.

Molecular pathway underlying CB1R-dependent modulation of I_h

What is the nature of the molecular pathway that links CB1Rs to postsynaptic I_h in SPCs? This question is especially interesting given that CB1Rs are traditionally considered to be primarily, albeit not exclusively, presynaptic (Bacci et al., 2004; Leterrier et al., 2006; Marinelli et al., 2009), whereas I_h in our experiments was a postsynaptic current. Because the CB1R is a G protein-coupled receptor, first we tested whether postsynaptic application of gallein (10μM, included in the whole-cell patch pipette), an inhibitor of the G protein βγ

subunit (Lehmann et al., 2008), was able to prevent the CB1R-dependent modulation of I_h. At baseline in SPCs, gallein reduced the sag amplitude compared to control, and subsequent WIN application did not increase the sag (Fig 3A; Table S1). In contrast, gallein did not affect sag amplitude in DPCs (Table S2). These results suggested that postsynaptic G-protein signaling was involved in the CB1R-I_h pathway.

CB1Rs can act through several mechanisms, including protein kinase cascades. The most common effect of CB1R activation is considered to be a decrease in cAMP levels (Howlett et al., 2004). However, decreased cAMP would be expected to cause a hyperpolarizing shift in I_h activation and a decreased sag response (He et al., 2014), i.e., the opposite of what we had observed. Moreover, the decreased cAMP levels induced by CB1R activation have been shown to be due to the $G\alpha_i$ subunit (Howlett et al., 2004), whereas the gallein effect suggests that the CB1R-I_h pathway is mediated by the $\beta\gamma$ subunit. Therefore, we considered possible alternatives. Interestingly, CB1Rs have been shown to activate mitogen activated protein kinases (MAPKs) of the c-Jun-N-terminal-Kinase family (JNKs; Turu and Hunyady, 2010), which, in turn, can increase cGMP through increased activation of nitric oxide synthase (NOS) and the nitric oxide- (NO-) related increase in the activity of guanylyl cyclase (GC) (Jones et al., 2008). The increase in cGMP would be then expected to cause a depolarizing shift in the activation curve for I_h. Note that HCNs can be gated by both cAMP and cGMP (He et al., 2014), and the cyclic nucleotide-binding domain of HCN1 reportedly exhibit comparable affinities toward cAMP and cGMP (Lolicato et al., 2011; but see DiFrancesco and Tortora, 1991). In order to test if JNKs are involved in the CB1R-I_h pathway, we applied the selective JNK inhibitor SP600125 (10μM) either extracellularly by bath application (JNK-inh-extra), or intracellularly in the postsynaptic recording pipette (JNK-inh-intra). Both treatments reduced the sag amplitude at baseline and abolished the effect of WIN on the sag in SPCs (Fig 3A; Table S1).

Next, we tested the effect of JNK activation by the postsynaptic, intra-pipette application of anisomycin (aniso-intra; 30μM), a protein-synthesis inhibitor that, in addition to other effects, is known to activate JNK (Turu and Hunyady, 2010). Consistent with increased JNK activation, aniso-intra increased sag amplitude in SPCs at baseline, occluded the sag amplitude-enhancing effect of WIN, and prevented the sag amplitude-decreasing effect of AM251. Extracellular JNK inhibition via bath application of SP600125 (JNK-inh-extra) was able to abolish the effect of anisomycin (Fig 3A; Table S1). Another MAPK modulator of I_h, p38 (Poolos et al, 2006), can be also activated by both CB1R and anisomycin (Turu and Hunyady, 2010), therefore, we tested the possible role of p38 in the CB1R-I_h pathway. Pre-incubation of slices with the p38 inhibitor SB203580 (p38-inh; 10μM) caused no changes in the baseline sag amplitude in SPCs or DPCs, and subsequent WIN application still increased sag in SPCs. In addition, the increased I_h induced by anisomycin was not affected by p38-inh (Fig 3A; Table S1). Taken together, these results suggest that postsynaptic CB1R activation increases JNK activity, resulting in enhancement of I_h in SPCs.

In contrast to SPCs, JNK-inh-extra or JNK-inh-intra did not reduce the sag amplitude at baseline in DPCs, indicating the JNK was not constitutively active in the latter cells (Table S2). However, JNK activation by aniso-intra did increase the baseline sag amplitude in DPCs (Table S2), suggesting that JNK was in fact present in DPCs, and, upon exogenous

activation, was able to modulate I_h in DPCs as well. There are different isoforms of JNKs in the brain. In order to determine which specific JNK isoform was involved in the CB1R-mediated regulation of postsynaptic I_h, we measured the baseline sag amplitude and the effects of CB1R modulation on sag in mice lacking either JNK1 (JNK1KO) or JNK2 (JNK2KO). The baseline sag amplitude was reduced in SPCs from JNK1KOs, and WIN did not potentiate the sag amplitude (Fig 3B; Table S1). In contrast, the sag response in DPCs was not altered in JNK1KOs (Table S2), and the sag amplitude at baseline in JNK1KOs was not different between SPCs and DPCs (Fig S1A and Table S1 and S2). These results showed that JNK1 played a major role in the CB1R-I_h pathway in SPCs.

Next, we examined the potential contribution of JNK2. The baseline sag amplitude in JNK2KOs was also significantly reduced compared to WT mice, however, this reduction was smaller compared to the reduction in JNK1KOs (Fig 3B). Similarly, WIN significantly increased the sag in SPCs in JNK2KOs, but the increase was smaller compared to the effect in their control littermates (in contrast, as described above, JNK1KOs completely lacked the WIN-induced increase in sag; Fig 3B, Table S1). As expected, the sag amplitude at baseline was not altered in the DPCs from JNK2KOs (Table S2). Taken together, these results reinforced the involvement of postsynaptic JNK in the CB1R-I_h pathway, and suggested a primary role for JNK1.

As mentioned above, JNK can enhance cGMP levels by increasing NOS activation (Jones et al., 2008), therefore, we examined the involvement of cGMP and NO in the CB1R-I_h pathway. Increase in cGMP levels is a well-documented consequence of NOS activation (Farinelli et al., 1996), and postsynaptic NO/cGMP increases enhance I_h in the hippocampus (Neitz et al., 2014). First, we tested the hypothesis that CB1R-mediated JNK activation increased postsynaptic I_h through the involvement of intracellular cGMP by including the selective and irreversible inhibitor of soluble GC (the enzyme responsible for cGMP production) 1H-[1,2,4]Oxadiazolo[4,3-a]quinoxalin-1-one (ODQ; 10μM) (Boulton et al., 1995) in the recording pipette. Postsynaptic application of ODQ reduced the sag amplitude at baseline, prevented the WIN-induced increase in sag and occluded the AM251-induced decrease in sag amplitude in SPCs. In addition, ODQ prevented the aniso-intra-induced increase in sag amplitude in SPCs (Fig 3C; Table S1). These results indicated that the CB1R-I_h pathway involved a JNK-induced increase in cGMP. In contrast, bath application of the selective adenylate cyclase inhibitor 2′,5′-dideoxyadenosine (DDOA; 15μM) (Pelkey et al., 2008) did not block the WIN-induced increase in sag, suggesting that the effect of WIN was not dependent on cAMP (Fig 3C, Table S1; importantly, DDOA did reduce the sag amplitude at baseline in SPCs, which served as a positive control for an effective reduction in intracellular cAMP levels). Second, we tested the involvement of NO by applying 2–4-carboxyphenyl-4,4,5,5-tetramethylimidazoline-1-oxyl-3-oxide (CPTIO), a specific NO scavenger. Pre-incubation followed by bath application of CPTIO (1mM) caused a significant decrease in the baseline sag amplitude in SPCs, and subsequent WIN application had no effect (Fig 3C; Table S1; note that postsynaptic, intracellular application of CPTIO at 10mM also significantly reduced the sag amplitude at baseline and decreased the effect of WIN; data not shown). Next, we analyzed the effect of bath application of NG-nitro-L-arginine methyl ester (L-NAME; 100μM), an inhibitor of NOS. Consistent with the CPTIO effect, L-NAME decreased the sag amplitude in SPCs at baseline and completely

prevented the sag-enhancing effect of WIN (Fig 3C; Table S1). Taken together, these experiments are consistent with the hypothesis that a JNK- and NOS-mediated cGMP increase is responsible for the I_h increase induced by CB1R activation (Fig. 3F).

2-AG is the endocannabinoid involved in the CB1R-I_h pathway

The fact that the CB1R antagonist and inverse agonist AM251, and the genetic deletion of the CB1Rs, decreased the baseline sag amplitude in SPCs indicated that the CB1R-I_h pathway was tonically active under our conditions. The tonic activity of the CB1R-I_h pathway could be due to constitutive (i.e., ligand-free) activity of CB1Rs and/or tonic activation of CB1Rs by endogenous ligands (Lee et al., 2015). The major endocannabinoids mediating CB1R-dependent central nervous system effects are 2-arachidonoylglycerol (2-AG) and anandamide, whose concentrations are controlled by their respective breakdown enzymes, monoacylglycerol lipase (MAGL) and fatty acid amide hydrolase (FAAH). Therefore, we used the MAGL inhibitor JZL184 (JZL; 100nM) and the FAAH inhibitor URB597 (URB; 1μM) to gain insight into which of these two major endocannabinoids might be involved in the endogenous activation of the CB1R-I_h pathway (note that JZL and URB at the concentrations used here have been recently demonstrated to cause robust, selective enhancement of 2-AG or anandamide levels, respectively, in hippocampal slices under the same conditions; Lee et al., 2015). Incubation of the slices in JZL significantly increased the baseline sag amplitude in SPCs, whereas application of URB had no effect (Fig 3D; Table S1). These data indicate that 2-AG is the main endogenous ligand that can contribute to the endogenous activation of the CB1R-I_h pathway.

CB1R-mediated modulation of postsynaptic I_h requires CB1Rs in glutamatergic cells

Next, we tested the cell type-specificity of the CB1Rs involved in the CB1R-I_h pathway. Because both glutamatergic and GABAergic cell populations express CB1Rs (Soltesz et al., 2015), we measured the sag amplitude at baseline and after WIN or AM251 application in slices from mice lacking CB1Rs from either GABAergic (GABA-CB1RKO) or glutamatergic (GLU-CB1RKO) cells (Monory et al., 2006). At baseline, the sag in SPCs from GLU-CB1RKOs was smaller than in WT controls, and WIN application did not increase the sag amplitude (Fig 3E; Table S1). In contrast, the sag amplitude at baseline in SPCs from GABA-CB1RKOs was similar to WT controls, and WIN application increased the sag (Fig 3E; Table S1). In addition, the sag at baseline in DPCs from both GLU-CB1RKO and GABA-CB1RKO animals was similar to WT control, and WIN did not exert any effect (Fig. 3E; Table S2). Note that the sag amplitude at baseline was similar in SPCs and DPCs in GLU-CB1RKOs but not in GABA-CB1RKOs (Fig S1A; Tables S1,S2). These results demonstrated that CB1Rs expressed specifically in glutamatergic cells mediate the CB1R-I_h pathway in SPCs. Note also that these data demonstrate that CB1Rs on presynaptic GABAergic terminals do not play a role in the cannabinoid regulation of postsynaptic I_h, in spite of the fact that these terminals express the highest numbers of CB1Rs (Dudok et al., 2015).

CB1R-I_h pathway requires postsynaptic CB1Rs expressed in SPCs

The results presented so far were consistent with a postsynaptically localized CB1R-I_h pathway, in contrast to classical presynaptic CB1R-mediated effects. Specifically, the fact

that the CB1R-I_h pathway was active in the presence of pharmacological blockade of major voltage-gated ion channels and ionotropic and metabotropic GABA and glutamate receptors suggested that presynaptic, CB1R-dependent modulation of action potential-dependent and independent neurotransmitter release was unlikely to be responsible for the CB1R-mediated modulation of I_h in SPCs. Moreover, the fact that intracellular, postsynaptic application of drugs targeting various steps in the CB1R-I_h pathway (Fig. 3F) was able to modulate I_h was also in agreement with a postsynaptic localization. In order to directly test whether the CB1R-I_h pathway is localized postsynaptically, we deleted CB1Rs from a subpopulation of CA1 PCs. Specifically, by injecting a retrograde, Cre-recombinase viral vector (Fig. 4A; see Experimental Procedures) in the medial entorhinal cortex (mEC) in CB1R-floxed mice, we were able to distinguish infected (i.e., red) CB1R lacking ($CB1R^-$) and neighboring, non-infected, $CB1R^+$ CA1 SPCs. Because of the lack of significant PC to PC glutamatergic connections in the CA1 (Bezaire and Soltesz, 2013), these experiments directly tested the role of postsynaptic CB1Rs in the CB1R-I_h pathway.

In $CB1R^-$ SPCs, the baseline sag amplitude was smaller than in $CB1R^+$ SPCs or in WT SPCs, and WIN application did not increase the sag in $CB1R^-$ SPCs (Fig 4B; Table S1). In contrast, the sag amplitude at baseline in $CB1R^+$ SPCs was similar to WT non-injected controls, and WIN application increased sag amplitude (Fig 4B; Table S1). As expected, the sag at baseline in DPCs from both $CB1R^+$ and $CB1R^-$ SPCs was similar to control, and WIN did not exert any effect on sag amplitude (Fig. 4B; Table S2). These results are consistent with a postsynaptic localization of the CB1Rs responsible for the CB1R-I_h pathway in SPCs.

CB1R-I_h pathway modulates the temporal summation of excitatory inputs to SPCs

Postsynaptic I_h plays a key role in controlling the integration of synaptic inputs in CA1 PCs, specifically by blunting the temporal summation of incoming excitatory postsynaptic events (Magee, 1999; Shah, 2014). Thus, we next examined whether the CB1R-I_h pathway modulates temporal summation. We recorded excitatory responses from Schaffer collaterals (SCs) in SPCs or DPCs using somatic whole-cell patch clamp techniques. We first examined the effects of WIN or AM251 on SC-evoked temporal summation of excitatory postsynaptic potentials (EPSPs) in SPCs or DPCs in WT mice. Repetitive stimulation (50 Hz, 5 pulses) of SCs gave rise to EPSPs that showed summation in both populations, measured as percentage of the ratio of the 5^{th} to 1^{st} EPSP amplitudes (Fig 5A–C). Importantly, WIN decreased the amplitude of the first EPSP to a similar extent in SPCs and DPCs (Figs 5A–C), indicating a similar degree of presynaptic CB1R-mediated inhibition of glutamate release onto SPCs and DPCs. However, in spite of the similar effect on the first EPSP, WIN reduced the magnitude of EPSP summation only in SPCs (Fig 5A left, B) but not in DPCs (Fig 5A right, C). Next, we tested the effect of AM251 on EPSP summation in WT mice. Application of AM251 increased the amplitude of the first EPSP to the same extent in SPCs and DPCs (compare Figs 5B to 5C), but increased EPSP summation only in SPCs (Fig 5A left, B) but not in DPCs (Fig 5A right, C).

As a next step, we analyzed CB1R modulation of temporal summation in SPCs in GLU-CB1RKO mice. At baseline, SPCs from the GLU-CB1RKOs showed increased summation

of EPSPs compared to their WT littermates (compare Figs 5A,B to 5D). Subsequent application of WIN or AM251 did not change the amplitude of the first EPSP and also had no effect on the magnitude of EPSP summation (Fig 5D right). To further confirm that the effect of CB1R modulation on temporal summation was indeed mediated by the postsynaptic CB1R-I_h pathway, we performed an additional set of experiments using retrograde Cre-virus-injected CB1R-floxed mice (as in Fig. 4A) and recorded the effect of CB1R modulation on temporal summation in selective $CB1R^-$ and $CB1R^+$ SPCs. At baseline, $CB1R^-$ SPCs showed increased summation of EPSPs compared to $CB1R^+$ SPCs (Fig 5E,F). In both $CB1R^+$ and $CB1R^-$ SPCs, subsequent application of WIN or AM251 changed the amplitude of the first EPSPs, but these drugs modulated the percentage of EPSP summation only in the $CB1R^+$ SPCs, whereas WIN and AM251 had no effect on the magnitude of EPSP summation in the $CB1R^-$ SPCs (Fig 5E,F).

Finally, we tested the role of the CB1R-I_h pathway on temporal summation of excitatory inputs in SPCs by analyzing the effect of CB1R modulation of excitatory inputs in HCN1KO mice and after pharmacological blockade of I_h with ZD7288 in WT. At baseline, SPCs from HCN1KOs and ZD7288-treated slices showed increased summation compared to their respective controls (Fig 5B,G,H), and subsequent application of WIN or AM251 had no effect on the magnitude of EPSP summation (Fig 5G, H). Importantly, WIN and AM251 were still able to modulate the amplitude of the first EPSP in both groups (Fig 5G,H), indicating intact presynaptic CB1R-mediated inhibition of neurotransmitter release. Taken together, these results demonstrated that the CB1R-I_h pathway regulates temporal summation of SC-induced EPSPs in SPCs. Furthermore, because of the similar effect of presynaptic CB1R modulation on glutamate release from SCs (as evidenced by the similar cannabinoid modulation of the first EPSPs) in SPCs, DPCs and in the SPCs where CB1Rs were selectively deleted, these data were also consistent with postsynaptically localized CB1Rs being responsible for the CB1-I_h pathway.

CB1Rs regulate LTP through I_h modulation

Because both CB1Rs and I_h can modulate LTP (Nolan et al., 2004; Stella et al., 1997), we examined the effect of pharmacological and genetic modulation of the CB1R-I_h pathway on LTP. In control conditions in whole cell-recorded SPCs from WT mice, theta-burst stimulation (TBS) of SCs induced reliable LTP, and as expected (Stella et al., 1997), WIN application blocked LTP induction (Fig 6A,F). In contrast, pharmacological blockade (AM251) or genetic ablation of CB1Rs from glutamatergic cells (GLU-CB1RKO) increased LTP (Fig 6A,B,F), and application of WIN in GLU-CB1RKOs did not exert any effect on LTP (Fig 6B,F). In general agreement with the key roles of CB1Rs on glutamatergic cells in mediating the CB1R-I_h pathway, LTP in GABA-CB1RKOs was similar to their control littermates and WIN application blocked LTP (Fig 6C,F). Next, in order to determine if the CB1R-I_h pathway was involved in the CB1R modulation of LTP, we used slices from HCN1KO and JNK1KO mice to show that LTP was enhanced in SPCs in both strains compared to their WT littermates (Fig 6D–F). Furthermore, the CB1R-induced modulation of LTP did not occur in HCN1KOs and JNK1KOs, suggesting that CB1Rs modulated LTP through the involvement of JNK1 and I_h (Fig 6D, E, F).

We also tested the role of the CB1R-I_h pathway on LTP induced with a different stimulation protocol. Pairing stimulation (PS) that combines low-frequency stimulation of SC with depolarization of SPCs (see Experimental Procedures) induced reliable LTP in SPCs in WT mice, and this LTP was sensitive to CB1R modulation (Fig S3A). In HCN1KO mice, PS-induced LTP was enhanced compared to WT, and insensitive to activation of CB1Rs (Fig S3B), similar to results from TBS stimulation.

The high density of HCN channels in the distal dendrites led us to hypothesize that the CB1R-I_h pathway would also influence LTP at the temporo-ammonic (TA) pathway, which synapses onto distal dendrites of CA1 PCs. Therefore, we induced LTP of the TA pathway with TBS and tested the effects of pharmacological or genetic modulation of the CB1R-I_h pathway. The results were similar to those from SC LTP. Stimulation of the TA pathway induced reliable LTP under control conditions, and WIN application blocked LTP induction (Fig 6G). In contrast, pharmacological (AM251) inhibition of CB1Rs significantly increased LTP (Fig 6G). Consistent with the role of CB1R-I_h pathway in modulating TA LTP, we found that LTP was enhanced in SPCs in HCN1KO mice compared to their WT littermates and that WIN application did not block TA LTP (Fig 6H), indicating that the CB1R-I_h pathway was involved in LTP at both SC and TA inputs. It should be noted that, in SC LTP experiments, WIN decreased the amplitude of the EPSCs at the baseline (i.e., before TBS or PS) similarly in WT, GABA-CB1RKO, JNK1KO and HCN1KO mice (% decrease: 16±2, 13±3, 15±1 and 14±2, respectively; no difference between strains), and the WIN-effect on the baseline EPSCs was also not different between WT and HCN1KO in the TA LTP experiments (% decrease: 9±1 and 11±2 respectively).

The CB1R-I_h pathway controls spatial memory consolidation

Next, to investigate if the CB1R-I_h pathway was responsible for cognitive impairments induced by CB1R agonists (Clarke et al., 2008), we used a spatial memory task, the object location memory test (OLM; Fig 7A) that is reportedly primarily hippocampus-dependent (Assini et al., 2009). Based on the role of the CB1R-I_h pathway in LTP, and cannabinoid-effects on memory processes (Clarke et al., 2008), we focused on memory consolidation by injecting animals with WIN (3mg/kg, i.p.) or vehicle immediately after the learning phase (Fig. 7A; given the relatively fast pharmacokinetics of WIN, the drug was not expected to be present at behaviorally relevant concentrations by the time testing took place 24 hours after WIN injection; McMahon and Koek, 2007). Note that, in order to focus on the memory-depressing role of WIN, we used a relatively long (10min) learning phase that yielded high discrimination index (DI) values (see Experimental Procedures) in vehicle-injected WT mice, indicative of robust learning; although this approach was ideal to study impairments in memory, it was not designed to investigate improvements in memory due to the already near-maximal DI value.

In WT mice, a single injection of WIN significantly decreased DI compared to vehicle (Fig 7B), demonstrating that WIN injected immediately after the learning (training) phase was able to disrupt consolidation of long-term spatial memory. Next, we used CB1RKO, GLU-CB1RKO, and GABA-CB1RKO animals and their respective WT control littermates to test if the memory impairment caused by WIN was mediated by CB1Rs expressed in

glutamatergic cells, the cell population that expressed the CB1Rs required for the CB1R-I_h pathway. Injection of WIN caused impairment in memory consolidation in WT controls and GABA-CB1RKOs, whereas WIN had no effect in CB1RKOs or GLU-CB1RKOs (Fig 7B). Therefore, the CB1Rs on glutamatergic cells were required for both the CB1R-I_h pathway and for the *in vivo* modulation of spatial memory consolidation by cannabinoids.

In addition, we also tested the link between WIN-induced spatial memory impairment and the CB1R-JNK-I_h pathway by determining the effect of WIN on spatial memory consolidation in JNK1KO mice, and after pharmacological (intrahippocampal injection of ZD7288) or genetic (HCN1KO) inhibition of I_h. WIN injection did not cause memory impairment in JNK1KOs, WT mice after intrahippocampal injection of ZD7288, or HCN1KOs (Fig 7B). Note that the total exploration time during both learning and testing phases was not different between the groups (Fig S4A,B). Taken together, these behavioral results demonstrated that HCN1 channels and JNK1 activation were necessary for long-term spatial memory impairment induced by cannabinoid administration.

Discussion

CB1Rs are abundantly expressed, yet highly selectively localized to specific excitatory and inhibitory cell types in the hippocampus and other cortical areas (Katona et al., 1999; Mackie, 2005; Soltesz et al., 2015). The highest number of CB1Rs is expressed by cholecystokinin (CCK)-expressing interneurons such as the perisomatically projecting CCK basket cells and the dendritically innervating Schaffer-collateral-associated cells (SCAs), whereas PCs appear to have lower levels of CB1R expression (Dudok et al., 2015). The primary function of CB1Rs is thought to be presynaptic, manifested as potent tonic or phasic inhibition of neurotransmitter release (Castillo et al., 2012). Interestingly, when comparisons were made between either glutamatergic and GABAergic boutons, or between perisomatic and dendritic GABAergic terminals, the absolute numbers of CB1Rs expressed by the particular axon terminal types did not correlate with the relative strength of CB1R-mediated inhibition of transmitter release, indicating that other factors, such as the presynaptic receptor to effector ratio (Dudok et al., 2015), may determine functional efficacy. The lack of a straightforward correspondence between CB1R numbers and their functional importance also has implications for the present study, since our results are most consistent with the hypothesis that, in contrast to the ‘classical’ presynaptic locus for CB1R-mediated effects on circuit excitability, the CB1R-I_h pathway that we identified in this study is primarily, if not exclusively, localized postsynaptically in the somatodendritic regions of the SPCs, where only a minority of the CB1Rs are thought to be expressed. The postsynaptic nature of the CB1R-I_h pathway was indicated by several lines of evidence. First, the CB1R-I_h pathway was fully functional even in the presence of blockers of voltage-gated Na^+, Ca^{2+} and K^+ channels, i.e. under conditions where there is a lack of action potential-dependent transmitter release. Second, the CB1R-mediated modulation of postsynaptic I_h was observed in the presence of antagonists of the major ionotropic and metabotropic GABA and glutamate receptors, indicating that it was unlikely that the classical inhibitory action of presynaptic CB1Rs on GABA or glutamate release resulted in a change in the activation levels of postsynaptic GABA or glutamate receptors leading to modulation of I_h. Third, although CB1Rs are particularly abundant on CCK interneurons that form perisomatic and

dendritic synapses on CA1 PCs, the CB1R-I_h pathway did not require CB1Rs on GABAergic neurons, as this pathway is intact in the GABA-CB1RKO mice. Fourth, postsynaptic, intra-pipette delivery of a variety of drugs (Fig. 3) were effective in modulating I_h in SPCs, consistent with the postsynaptic localization of the CB1R-I_h pathway. It should be noted here that each individual step in the CB1R-I_h pathway has been identified in prior studies. For example, endogenous or exogenous cannabinoid activation of CB1Rs in cerebral cortical slices had been shown to increase phosphorylation and activity of JNK (Turu and Hunyady, 2010), and JNK activation, in turn, can increase NO levels (Guan et al., 1999) and subsequently enhance intracellular cGMP (Jones et al., 2008). Similarly, the effect of NO/cGMP on I_h is well documented (Neitz et al., 2014) and involves direct interaction between cGMP and HCN channels that causes a small (3–4 mV), but functionally important depolarizing shift in I_h activation (He et al., 2014). Note that the steepness of the activation curve for I_h means that even a small change in V_{50} can result in a relatively large functional effect (Chen et al., 2001; Shah, 2014). Fifth, the most direct evidence that indicated the postsynaptic localization of the CB1Rs involved in the CB1R-I_h pathway came from results showing that the retrograde, viral deletion of CB1Rs in a subpopulation of CA1 PCs (Fig 4A) (i.e. the postsynaptic cells in our paradigm) was sufficient to abolish the effect of CB1R modulation of postsynaptic I_h.

Taken together, these data demonstrated a molecular mechanism linking CB1Rs to dendritic I_h, and that the CB1Rs involved in this pathway were expressed postsynaptically by glutamatergic principal cells. There is also considerable evidence for the postsynaptic, somatodendritic localization of a proportion of plasma membrane CB1Rs (Bacci et al., 2004; Leterrier et al., 2006; Marinelli et al., 2009; Simon et al., 2013). In fact, kinetic analysis in hippocampal cell cultures revealed that the majority of the newly synthesized CB1Rs appear first on the somatodendritic plasma membrane, from which they are subsequently removed by on-going endocytosis before being delivered to the axons where they accumulate (Leterrier et al., 2006). While the proportion of CB1Rs expressed on the plasma membrane in the somatodendritic compartment has been reported to be only 10 to 20% of the total receptor population, endocytosis of the somatodendritically expressed CB1Rs was shown to be required for the proper axonal targeting of the CB1Rs (Leterrier et al., 2006; Simon et al., 2013). These transient dendritic plasmamembrane CB1Rs were found to be constitutively active, and, although endocytosed at a relatively high rate, they were still able to modulate second messenger pathways (Leterrier et al., 2006; Simon et al., 2013). Importantly, somatodendritic CB1Rs have also been shown to play key roles in endocannabinoid-dependent short-term plasticity of intrinsic excitability in specific subsets of interneurons and PCs in acute cortical slices, where a train of action potentials leads to the release of endocannabinoids that appear to bind to CB1Rs on the same cell in an autocrine fashion, resulting in a robust hyperpolarization of the cell membrane through a pathway involving GIRK channels (Bacci et al., 2004; Marinelli et al., 2009).

Cell type-specificity of the CB1R-I_h signaling pathway

Our results demonstrate that the CB1R-I_h pathway was functional only in the SPCs, but not in their neighboring DPC counterparts located only a few tens of microns away. These data were in general agreement with accumulating evidence for the presence of robust

developmental, gene expression, morphological, synaptic connectivity and functional differences between CA1 SPCs and DPCs (Lee et al., 2014; Mizuseki et al., 2011). In terms of structural differences, SPCs have larger basal dendritic trees, and they form excitatory connections with fast spiking, parvalbumin-expressing basket cells (PVBCs) with significantly higher probability than their DPC counterparts (Lee et al., 2014); however, SPCs receive markedly weaker inhibitory inputs from PVBCs, indicating that these two PC populations participate in distinct local excitatory-inhibitory microcircuits (Lee et al., 2014). The SPCs also differ from DPCs in their intrinsic membrane excitability, displaying more depolarized resting membrane potentials and larger sag responses to hyperpolarizing current pulses indicative of larger I_h (Lee et al., 2014), in agreement with our results (Figs 1,2). However, it should be noted that while I_h was smaller in the DPCs, it was still present in the latter cells as well, raising the question as to why CB1R activation was ineffective in enhancing I_h in DPCs. This question is particularly interesting in light of the fact that CB1R agonist application decreased the first EPSP to the same extent in SPCs and DPCs, indicating that presynaptic CB1Rs were expressed and similarly efficacious on the SC terminals that innervate the two cell populations. Our results indicated that the difference between SPCs and DPCs in terms of the CB1R-I_h pathway was upstream from JNK, because aniso-intra, a JNK activator, was able to enhance I_h not only in SPCs but also in DPCs, with the percent potentiation being similar in the two cell types. Although the precise mechanism underlying the striking cell type-specificity of the CB1R-mediated modulation of I_h in SPCs and DPCs is not yet fully understood, our data demonstrated that the CB1R-I_h pathway was in fact the key determinant of the differential I_h amplitude in these two distinct PC populations. This surprising conclusion was supported by the observations that a variety of manipulations that inhibited the CB1R-I_h pathway, including bath application of AM251, gallein, CPTIO, L-NAME, use of GLU-CB1RKOs or JNK1KOs, selective deletion of CB1Rs in a subpopulation of CA1 PCs and the intra-pipette application of either JNK-inh or ODQ, all specifically reduced I_h only in SPCs, and, critically, abolished the difference in sag response and I_h between the SPCs and DPCs. These data indicated that a tonically active CB1R-I_h pathway was exclusively responsible for maintaining the larger I_h in SPCs, and that tonic activation of this pathway was absent from the DPCs.

Functional implications and outlook

The CB1Rs and HCNs have been reported to play important roles in an unusual diversity of physiological processes within and outside of the nervous system, and both have also been implicated in various neurological and psychiatric disorders (Katona and Freund, 2008; Soltesz et al., 2015; He et al., 2014; Shah, 2014). In spite of these diverse effects, however, CB1Rs and HCNs have been reported to exert similar modulation of long-term synaptic plasticity and learning and memory (Nolan et al., 2004; Zhu, 2006). Our results revealed a previously unknown link between these two seemingly unrelated key molecules, in the form of a new mechanism of cannabinoid regulation that is postsynaptic in nature and involves HCN1 channels. The CB1R-I_h pathway appears to be able to exert functional effects at several distinct levels, from dendritic temporal integration of synaptic inputs to long-term synaptic plasticity and spatial learning. While the involvement of the CB1R-I_h pathway in spatial memory was hippocampus-dependent (as indicated by the fact that injection of the I_h inhibitor ZD7288 into the hippocampus was sufficient to block the memory-depressing

effects of systemically injected cannabinoid ligands), it should be noted that the pathway may also be active in other brain areas as well, possibly expressed in select subpopulations of principal cells with specific circuit function. An interesting aspect of the CB1R-I_h pathway was that it was activated tonically in CA1 SPCs, which made bidirectional modulation possible. For example, not only the activation of CB1Rs resulted in markedly reduced I_h-dependent temporal summation and LTP, but the inhibition of the tonic activity of CB1Rs with AM251 was able to exert the opposite effects, i.e., enhancement of temporal summation and LTP through HCN1 modulation. Our results with the pharmacological inhibition of the endocannabinoid metabolic enzymes indicated that the major endogenous ligand 2-AG can modulate the CB1R-I_h pathway, however, contribution from the constitutive (ligand-free) activity of the CB1R is also possible (Lee et al., 2015). Endogenous regulation of tonic CB1R activity has recently received increased attention due to its possible involvement in several major disorders, including autism, Huntington's disease and epilepsy (for references, see Soltesz et al., 2015).

Interestingly, the CB1R-I_h pathway was able to robustly modulate LTP and spatial memory in spite of being active only in the SPCs. However, it should be noted that DPCs have higher firing rates, burst more frequently, and are more likely to have place fields (Mizuseki et al., 2011), therefore, it is possible that SPCs exerted their CB1R-I_h pathway-dependent effects on memory at least partially through the involvement of DPCs (Lee et al., 2014). Future research will be necessary to investigate the interesting possibility that the CB1R-I_h pathway may also be involved in the presynaptic regulation of glutamate and GABA release at select synapses where the functional involvement of I_h had been observed (Huang and Trussell, 2014; Huang et al., 2011). Finally, our findings are likely to be of considerable relevance for understanding cannabinoid-effects on cognition in the normal brain as well as for the cannabinoid control of pathological neuronal activity patterns in neurological and psychiatric disorders such as catastrophic epilepsies of infancy and other diseases (Katona and Freund, 2008; Soltesz et al., 2015).

EXPERIMENTAL PROCEDURES

Mice

All animal procedures were performed in accordance with the Institutional Animal Care and Use Committee (IACUC) at University of California, Irvine, and with the Administrative Panel on Laboratory Animal Care (APLAC) at Stanford University.

Three to ten week old male mice of the following strains were used. **CB1R mutants**: CB1RKO (RRID:MGI_3045437), GLU-CB1RKO (RRID:MGI_3758333), GABA-CB1RKO (RRID:MGI_3758334) (see Monory et al., 2006), Ai9/CB1R$^{f/f}$ (RRID:MGI_3831871) and respective WT littermates. For selective deletion of CB1Rs from subpopulations of CA1 PCs, see Supplemental Experimental Procedures. **HCN1 mutants**: Forebrain-specific HCN1KO (see Nolan et al., 2003; RRID:MGI_2686969). **JNK mutants**: B6129S1-Mapk8^{tm1Flv}/J mice lacking *JNK1* (JNK1KO; RRID:IMSR_JAX:004319) and B6.129S2-Mapk9^{tmFlv}/J mice lacking *JNK2* (JNK2KO; RRID:IMSR_JAX:004321). Animals were housed in a temperature- and humidity-controlled room with a 12:12 h light-

dark cycle, and had access to food and water *ad libitum*. For addition information, see Supplemental Experimental Procedures.

Pharmacological agents

WIN55,212 (WIN: *in vitro*: 0.5μM; *in vivo*: 3mg/kg), AM251 (10μM), ZD7288 (*in vitro*: 0.1mM; *in vivo*: 15μg/animal), SB203580 (p38-inhibitor; 10μM), SP600125 (JNK-inhibitor; 10μM), JZL184 (JZL; 1μM), URB597 (URB; 1μM), gallein (10μM), anisomycin (30μM), ODQ (10μM), L-NAME (100μM), DDOA (10mM) were obtained from Tocris (Ellisville, MO). CPTIO (1mM or 10mM) was obtained from Cayman (Ann. Arbor, MI).

In vitro electrophysiology

Coronal hippocampal slices (300μm) were prepared from the dorsal hippocampus of 3–10 week old mice, and sections −1.9 to 2.5 mm anterior-posterior with respect to bregma were used. Slices were incubated in sucrose-containing artificial cerebrospinal fluid (ACSF) for 2 to 3 hours, then transferred into ACSF used for recordings (33°C). Drugs modulating the CB1R-I_h pathway were added either to the perfusate or intra-pipette recording solution, as specified in the Results. Sag measurements were obtained using whole cell recordings in current-clamp configuration (holding potential: −70mV; patch pipettes: 3–5MΩ) and hyperpolarizing current injections (2s steps, −400 to −50pA with 50pA increments). Input resistance was measured from voltage responses to small current pulses (2s steps, −100pA to −50pA, 50pA increments) at steady state (0.8s–1.0s from start of current steps). For dendritic I_h measurements cell-attached patch-clamp recordings were obtained in voltage-clamp configuration (200–250μm from soma, seal resistance >5GΩ) using pipettes (4–6MΩ) fire-polished on a microforge (Narishige, Tokyo, Japan) and by applying 1s step hyperpolarizations from a holding potential of ~−30mV from V_m in −10mV increments (−40 to −120mV). Activation curves were obtained as described (Magee et al., 1998; Dyhrfjeld-Johnsen et al., 2009). For temporal summation experiments, a train of EPSPs (~3mV, using 5 pulses at 50Hz, 0.12ms every 20s) was evoked in control conditions and after WIN or AM251. The magnitude of the summation was measured as the ratio of the 5^{th} over the 1^{st} EPSP amplitude. For LTP, a concentric bipolar stimulating electrode was placed in stratum radiatum (for SC-LTP) or stratum lacunosum moleculare (for TA-LTP), and EPSCs (~50% of maximum, every 60s) were recorded. First, to determine the effects of the drugs on EPSCs, 20min pre- and post-drug recordings were obtained (the post-drug recordings were used as baseline for LTP experiments). For TBS, 4 theta-burst trains (1s, containing 5 bursts of 10 stimuli at 100Hz) at 20s intervals were delivered, and EPSCs were recorded for additional 60 min. For the PS-induced LTP of the SC, 200 pulses at 1 Hz were applied, coupled with depolarizing voltage clamp pulses (50ms). For additional information, see Supplemental Experimental Procedures.

Soma location identification

After *in vitro* recording with pipettes containing biocytin, slices were transferred into a fixative solution. Slices were resectioned at 70μm, and streptavidin conjugated to Alexa 350 (Invitrogen; 1:500) or DyLight 594 (Jackson Immunoresearch; 1:500) were used to visualize

biocytin-filled cells. Post-hoc identified CA1 PCs were categorized as SPCs or DPCs, see Supplemental Experimental Procedures.

Viral Injections

Intracerebral injection of the AAV vector into the mEC of Ai9/CB1R$^{f/f}$ mice was performed stereotaxically under isoflurane anesthesia. The AAV-EF1a-mCherry-IRES-WGA-Cre (1µl at 0.1µl/min) was delivered using an injection pump (World Precision Instrument, Inc, Sarasota, FL, USA; model 504127). After recovery, animals were returned to their home cage in the vivarium for at least 4 weeks; see Supplemental Experimental Procedures.

Behavioral Experiments

The OLM task was performed as described in Roozendaal et al., 2010 and McQuown et al., 2011. Briefly, during training phase, two identical objects were presented to the animals for 10 min (learning phase). Immediately after, mice were injected with WIN (3mg/kg, i.p.) or vehicle. After 24h, spatial memory was tested for 5min (test phase), during which one of the objects was moved to a novel location (Fig 7A). Videos were analyzed and the discrimination index (DI= {[time spent exploring object in novel location–time spent exploring object in familiar location]/total time exploring both objects} × 100) during the test phase was calculated as a measure of spatial memory. Total exploration time during learning and testing was also determined. For additional information, see Supplemental Experimental Procedures.

Statistical Analysis

Paired or unpaired two-tailed Student's t-tests (Figs 3, 4) and ANOVA (all other figures) were used. ANOVAs were followed by Tukey-Kramer tests for mean comparisons. Data are presented as mean ± SE. A p-value < 0.05 was considered significant.

Supplementary Material

Refer to Web version on PubMed Central for supplementary material.

Acknowledgments

We thank K. Mackie for providing JNK KO mice; S. Siegelbaum for providing the forebrain-restricted HCN1KO mice; G. Marsicano for providing the GLU-, GABA- and global-CB1RKO mice; T. Nguyen and S. Felong for technical support. This work was supported by the U.S. National Institutes of Health (NS35915 and NS94668 to I.S.; F31NS086429 to A.B., R25NS065741-04S1 to A.A.) and National Aeronautics and Space Administration (NSCOR NNX10AD59G to I.S.), and by a European Molecular Biology Organization (EMBO) long-term fellowship to M.M..

REFERENCES

Assini FL, Duzzioni M, Takahashi RN. Object location memory in mice: pharmacological validation and further evidence of hippocampal CA1 participation. Behavioural brain research. 2009; 204:206–211. [PubMed: 19523494]

Bacci A, Huguenard JR, Prince DA. Long-lasting self-inhibition of neocortical interneurons mediated by endocannabinoids. Nature. 2004; 431:312–316. [PubMed: 15372034]

Basavarajappa BS, Subbanna S. CB1 receptor-mediated signaling underlies the hippocampal synaptic, learning, and memory deficits following treatment with JWH-081, a new component of spice/K2 preparations. Hippocampus. 2014; 24:178–188. [PubMed: 24123667]

Bezaire MJ, Soltesz I. Quantitative assessment of CA1 local circuits: knowledge base for interneuron-pyramidal cell connectivity. Hippocampus. 2013; 23:751–785. [PubMed: 23674373]

Boulton CL, Southam E, Garthwaite J. Nitric oxide-dependent long-term potentiation is blocked by a specific inhibitor of soluble guanylyl cyclase. Neuroscience. 1995; 69:699–703. [PubMed: 8596640]

Castillo PE, Younts TJ, Chavez AE, Hashimotodani Y. Endocannabinoid signaling and synaptic function. Neuron. 2012; 76:70–81. [PubMed: 23040807]

Chen K, Aradi I, Thon N, Eghbal-Ahmadi M, Baram TZ, Soltesz I. Persistently modified h-channels after complex febrile seizures convert the seizure-induced enhancement of inhibition to hyperexcitability. Nature medicine. 2001; 7:331–337.

Chen K, Ratzliff A, Hilgenberg L, Gulyas A, Freund TF, Smith M, Dinh TP, Piomelli D, Mackie K, Soltesz I. Long-term plasticity of endocannabinoid signaling induced by developmental febrile seizures. Neuron. 2003; 39:599–611. [PubMed: 12925275]

Clarke JR, Rossato JI, Monteiro S, Bevilaqua LR, Izquierdo I, Cammarota M. Posttraining activation of CB1 cannabinoid receptors in the CA1 region of the dorsal hippocampus impairs object recognition long-term memory. Neurobiol Learn Mem. 2008; 90:374–381. [PubMed: 18524639]

Curtin JF, Cotter TG. Anisomycin activates JNK and sensitises DU 145 prostate carcinoma cells to Fas mediated apoptosis. British journal of cancer. 2002; 87:1188–1194. [PubMed: 12402161]

Di Francesco D, Tortora P. Direct activation of cardiac pacemaker channels by intracellular cyclic AMP. Nature. 1991; 9(351):145–147.

Dyhrfjeld-Johnsen J, Morgan RJ, Soltesz I. Double Trouble? Potential for Hyperexcitability Following Both Channelopathic up- and Downregulation of I(h) in Epilepsy. Frontiers in neuroscience. 2009; 3:25–33. [PubMed: 19753094]

Dudok B, Barna L, Ledri M, Szabo SI, Szabadits E, Pinter B, Woodhams SG, Henstridge CM, Balla GY, Nyilas R, et al. Cell-specific STORM super-resolution imaging reveals nanoscale organization of cannabinoid signaling. Nature neuroscience. 2015; 18:75–86. [PubMed: 25485758]

Farinelli SE, Park DS, Greene LA. Nitric oxide delays the death of trophic factor-deprived PC12 cells and sympathetic neurons by a cGMP-mediated mechanism. The Journal of neuroscience : the official journal of the Society for Neuroscience. 1996; 16:2325–2334. [PubMed: 8601812]

He C, Chen F, Li B, Hu Z. Neurophysiology of HCN channels: from cellular functions to multiple regulations. Progress in neurobiology. 2014; 112:1–23. [PubMed: 24184323]

Herrmann S, Hofmann F, Stieber J, Ludwig A. HCN channels in the heart: lessons from mouse mutants. Br J Pharmacol. 2012; 166:501–509. [PubMed: 22141457]

Howlett AC. Efficacy in CB1 receptor-mediated signal transduction. Br J Pharmacol. 2004; 142:1209–1218. [PubMed: 15308578]

Huang H, Trussell LO. Presynaptic HCN channels regulate vesicular glutamate transport. Neuron. 2014; 84:340–346. [PubMed: 25263752]

Huang Z, Lujan R, Kadurin I, Uebele VN, Renger JJ, Dolphin AC, Shah MM. Presynaptic HCN1 channels regulate Cav3.2 activity and neurotransmission at select cortical synapses. Nature neuroscience. 2011; 14:478–486. [PubMed: 21358644]

Jarsky T, Mady R, Kennedy B, Spruston N. Distribution of bursting neurons in the CA1 region and the subiculum of the rat hippocampus. The Journal of comparative neurology. 2008; 506:535–547. [PubMed: 18067146]

Jones JD, Carney ST, Vrana KE, Norford DC, Howlett AC. Cannabinoid receptor-mediated translocation of NO-sensitive guanylyl cyclase and production of cyclic GMP in neuronal cells. Neuropharmacology. 2008; 54:23–30. [PubMed: 17707868]

Katona I, Freund TF. Endocannabinoid signaling as a synaptic circuit breaker in neurological disease. Nature medicine. 2008; 14:923–930.

Katona I, Sperlagh B, Sik A, Kafalvi A, Vizi ES, Mackie K, Freund TF. Presynaptically located CB1 cannabinoid receptors regulate GABA release from axon terminals of specific hippocampal

interneurons. The Journal of neuroscience : the official journal of the Society for Neuroscience. 1999; 19:4544–4558. [PubMed: 10341254]

Kleppisch T, Wolfsgruber W, Feil S, Allmann R, Wotjak CT, Goebbels S, Nave KA, Hofmann F, Feil R. Hippocampal cGMP-dependent protein kinase I supports an age- and protein synthesis-dependent component of long-term potentiation but is not essential for spatial reference and contextual memory. The Journal of neuroscience : the official journal of the Society for Neuroscience. 2003; 23:6005–6012. [PubMed: 12853418]

Lee SH, Marchionni I, Bezaire M, Varga C, Danielson N, Lovett-Barron M, Losonczy A, Soltesz I. Parvalbumin-positive basket cells differentiate among hippocampal pyramidal cells. Neuron. 2014; 82:1129–1144. [PubMed: 24836505]

Lee, SH.; Ledri, M.; Toth, B.; Marchionni, I.; Henstridge, CM.; Dudok, B.; Szabo, SI.; Renkecz, T.; Oberoi, M.; Watanabe, M.; Limoli, CL.; Horovai, G.; Soltesz, I.; Katona, I. The Journal of Neuroscience : the official journal of the Society for Neuroscience. 2015. Multiple form of endocannabinoid and endovanilliod signaling regulate the tonic control of GABA release. In press

Lehmann DM, Seneviratne AM, Smrcka AV. Small molecule disruption of G protein beta gamma subunit signaling inhibits neutrophil chemotaxis and inflammation. Molecular pharmacology. 2008; 73:410–418. [PubMed: 18006643]

Leterrier C, Laine J, Darmon M, Boudin H, Rossier J, Lenkei Z. Constitutive activation drives compartment-selective endocytosis and axonal targeting of type 1 cannabinoid receptors. The Journal of neuroscience : the official journal of the Society for Neuroscience. 2006; 26:3141–3153. [PubMed: 16554465]

Lolicato M, Nardini M, Gazzarini S, Moller S, Berrtinetti D, Herberg FW, Bolognesi M, Martin H, Fasolini M, Bertrand JHA, Arrigoni C, Thiel G, Moroni A. Tetramerization dynamics of C-terminal domain underlies isoform-specific cAMP gating in Hyperpolarization-activated cyclic nucleotide-gated channels. Journal of Biological Chemistry. 2011; 286(52):44811–44820. [PubMed: 22006928]

Mackie K. Distribution of cannabinoid receptors in the central and peripheral nervous system. Handbook of experimental pharmacology. 2005:299–325. [PubMed: 16596779]

Magee JC. Dendritic hyperpolarization-activated currents modify the integrative properties of hippocampal CA1 pyramidal neurons. The Journal of neuroscience : the official journal of the Society for Neuroscience. 1998; 18:7613–7624. [PubMed: 9742133]

Marinelli S, Pacioni S, Cannich A, Marsicano G, Bacci A. Self-modulation of neocortical pyramidal neurons by endocannabinoids. Nature neuroscience. 2009; 12:1488–1490. [PubMed: 19915567]

Marsicano G, Goodenough S, Monory K, Hermann H, Eder M, Cannich A, Azad SC, Cascio MG, Gutierrez SO, van der Stelt M, et al. CB1 cannabinoid receptors and on-demand defense against excitotoxicity. Science. 2003; 302:84–88. [PubMed: 14526074]

McMahon LR, Koek W. Differences in the relative potency of SR 141716A and AM 251 as antagonists of various in vivo effects of cannabinoid agonists in C57BL/6J mice. Eur J Pharmacol. 2007; 569:70–76. [PubMed: 17553486]

McQuown SC, Barrett RM, Matheos DP, Post RJ, Rogge GA, Alenghat T, Mullican SE, Jones S, Rusche JR, Lazar MA, et al. HDAC3 is a critical negative regulator of long-term memory formation. The Journal of neuroscience : the official journal of the Society for Neuroscience. 2011; 31:764–774. [PubMed: 21228185]

Metna-Laurent M, Marsicano G. Rising stars: modulation of brain functions by astroglial type-1 cannabinoid receptors. Glia. 2015; 63:353–364. [PubMed: 25452006]

Mizuseki K, Diba K, Pastalkova E, Buzsaki G. Hippocampal CA1 pyramidal cells form functionally distinct sublayers. Nature neuroscience. 2011; 14:1174–1181. [PubMed: 21822270]

Monory K, Massa F, Egertova M, Eder M, Blaudzun H, Westenbroek R, Kelsch W, Jacob W, Marsch R, Ekker M, et al. The endocannabinoid system controls key epileptogenic circuits in the hippocampus. Neuron. 2006; 51:455–466. [PubMed: 16908411]

Neitz A, Mergia E, Imbrosci B, Petrasch-Parwez E, Eysel UT, Koesling D, Mittmann T. Postsynaptc NO/cGMP increases NMDA receptor currents via hyperpolarization-activated cyclic nucleotide-gated channels in the hippocampus. Cerebral Cortex. 2014; 24:1923–1936. [PubMed: 23448871]

Nolan MF, Malleret G, Dudman JT, Buhl DL, Santoro B, Gibbs E, Vronskaya S, Buzsaki G, Siegelbaum SA, Kandel ER, et al. A behavioral role for dendritic integration: HCN1 channels constrain spatial memory and plasticity at inputs to distal dendrites of CA1 pyramidal neurons. Cell. 2004; 119:719–732. [PubMed: 15550252]

Pelkey KA, Topolnik L, Yuan XQ, Lacaille JC, McBain CJ. State-dependent cAMP sensitivity of presynaptic function underlies metaplasticity in a hippocampal feedforward inhibitory circuit. Neuron. 2008; 60:980–987. [PubMed: 19109906]

Poolos NP, Bullis JB, Roth MK. Modulation of h-channels in hippocampal pyramidal neurons by p38 mitogen-activated protein kinase. The Journal of neuroscience : the official journal of the Society for Neuroscience. 2006; 26:7995–8003. [PubMed: 16870744]

Roozendaal B, Hernandez A, Cabrera SM, Hagewoud R, Malvaez M, Stefanko DP, Haettig J, Wood MA. Membrane-associated glucocorticoid activity is necessary for modulation of long-term memory via chromatin modification. The Journal of neuroscience : the official journal of the Society for Neuroscience. 2010; 30:5037–5046. [PubMed: 20371824]

Shah MM. Cortical HCN channels: function, trafficking and plasticity. The Journal of physiology. 2014; 592:2711–2719. [PubMed: 24756635]

Simon AC, Loverdo C, Gaffuri AL, Urbanski M, Ladarre D, Carrel D, Rivals I, Leterrier C, Benichou O, Dournaud P, et al. Activation-dependent plasticity of polarized GPCR distribution on the neuronal surface. J Mol Cell Biol. 2013; 5:250–265. [PubMed: 23585691]

Soltesz I, Alger BE, Kano M, Lee SH, Lovinger DM, Ohno-Shosaku T, Watanabe M. Weeding out bad waves: towards selective cannabinoid circuit control in epilepsy. Nature reviews Neuroscience. 2015; 16:264–277. [PubMed: 25891509]

Stella N, Schweitzer P, Piomelli D. A second endogenous cannabinoid that modulates long-term potentiation. Nature. 1997; 388:773–778. [PubMed: 9285589]

Turu G, Hunyady L. Signal transduction of the CB1 cannabinoid receptor. J Mol Endocrinol. 2010; 44:75–85. [PubMed: 19620237]

Zhu PJ. Endocannabinoid signaling and synaptic plasticity in the brain. Crit Rev Neurobiol. 2006; 18:113–124. [PubMed: 17725514]

Highlights

1. Cannabinoid type-1 receptors (CB1Rs) modulate the key dendritic current I_h
2. The CB1R-I_h pathway is present in superficial but not deep CA1 pyramidal cells
3. CB1Rs involved in this pathway are postsynaptic and act through JNK, NO and cGMP
4. The pathway is critical for cannabinoid effects on LTP and spatial memory

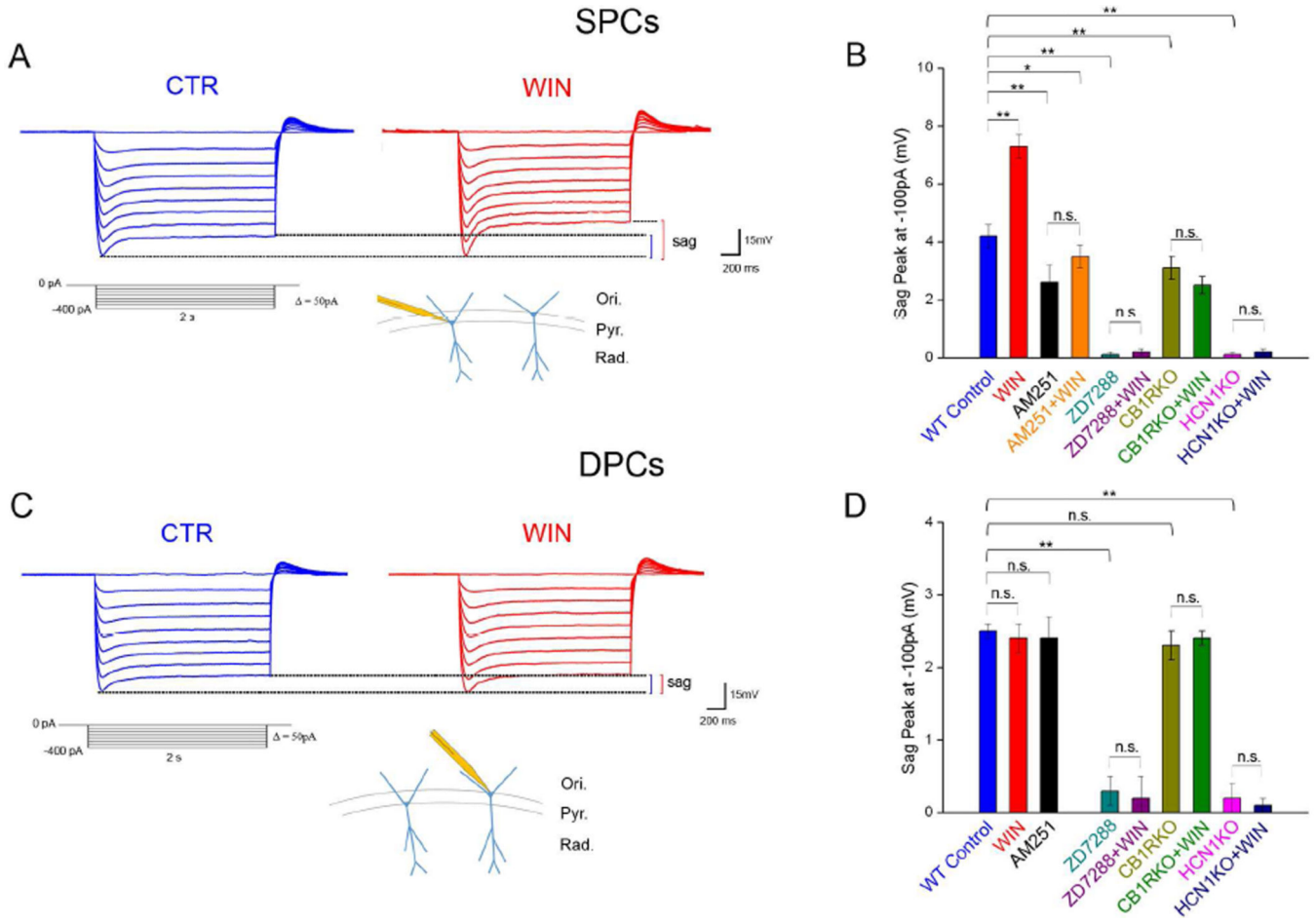

Figure 1. Effects of CB1R modulation on sag in SPCs and DPCs

A) Top: Examples of sag potentials from an SPC (2 sec pulses, −400pA to 0pA, 50pA steps) before (CTR, blue) and 4 min after WIN application (red). Bottom: Hyperpolarizing step protocol and schematic representation of SPCs in the CA1.

B) Effects of pharmacological and genetic modulation of CB1Rs and/or HCNs on sag amplitude recorded at −100 pA in SPCs (n of cells: WT Control: 11; WIN: 11; AM251: 13; AM251+WIN: 13; ZD7288: 12; ZD7288+WIN: 13; CB1RKO: 13; CB1RKO+WIN: 12; HCN1KO: 12; HCN1KO+WIN: 11; for all current steps, see Table S1).

C) Example of sag potentials a DPC (as in A).

D) Effects of pharmacological and genetic modulation of CB1Rs and/or HCNs on sag amplitude recorded at −100 pA in DPCs (n: WT Control: 13; WIN: 15; AM251: 12; ZD7288: 14; ZD7288+WIN: 12; CB1RKO: 13; CB1RKO+WIN: 13; HCN1KO: 15; HCN1KO+WIN: 15; see Table S2).

Data in this and subsequent figures are represented as mean±standard error (SE); n.s.: not significant; *p<0.05; **p<0.01. Ori: stratum oriens; Pyr: stratum pyramidale; Rad: stratum radiatum.

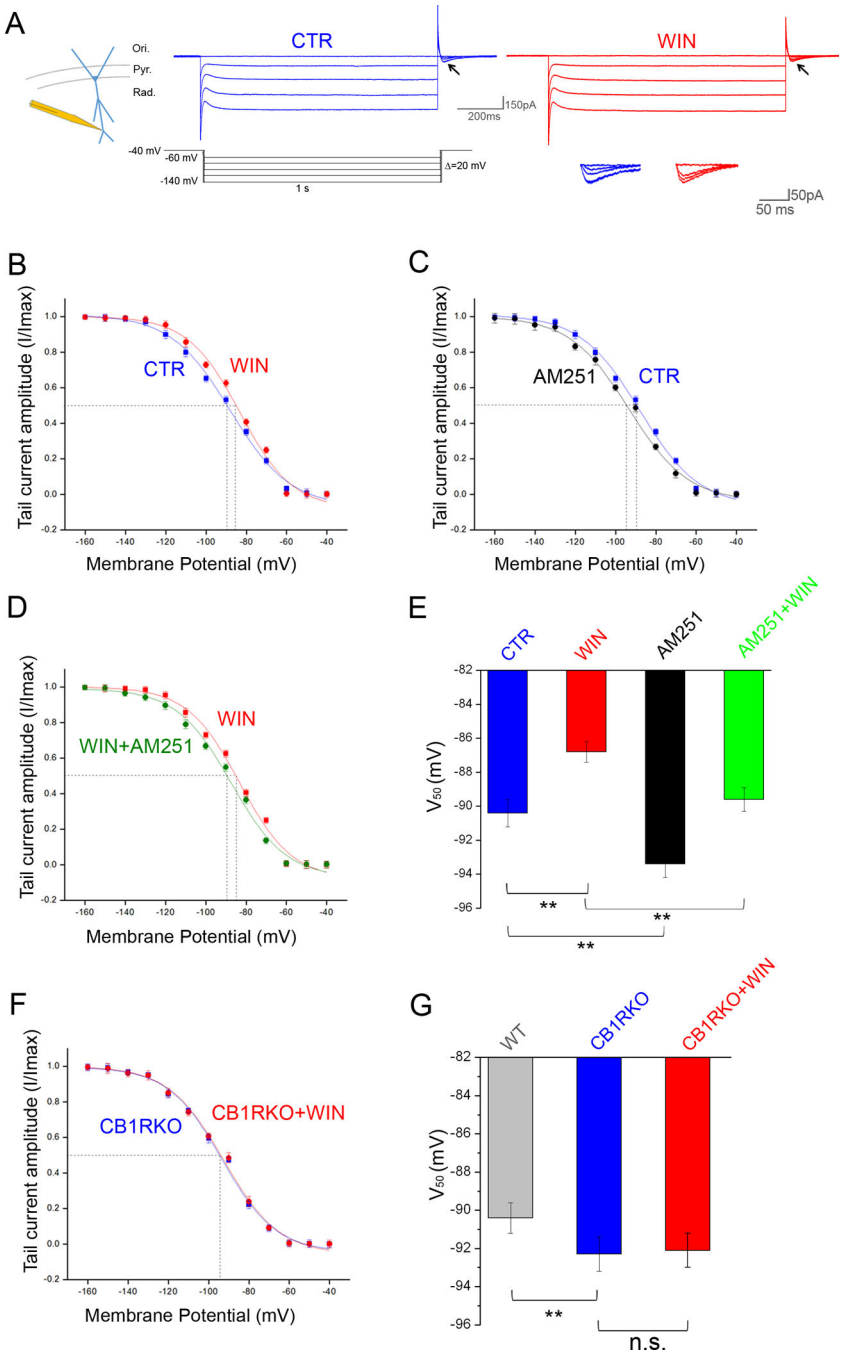

Figure 2. Effects of CB1R modulation on I_h activation in SPCs

A) Example traces of I_h from cell-attached patches from distal dendrites of SPCs (~250–300 μm from soma) under control conditions (CTR, blue) or after perfusion with WIN (red). Enlargements of the tail currents (arrows) are shown in the inset.

B) I_h activation (determined from tail currents; inset) in SPCs from WT animals in control condition and after WIN application; n: CTR 12; WIN 14; see Table S3 for raw values.

C) I_h activation in SPCs from WT animals in CTR and after AM251 application; n: CTR: 12; AM251: 11; see Table S3 for raw values.

D) I_h activation in SPCs from WT animals treated with WIN or with WIN+AM251; n=12 for both; see Table S3 for raw values.

E) Summary data of V_{50} values measured in the four different conditions depicted in panels B to D.

F) I_h activation in SPCs from CB1RKO animals in control conditions and after WIN application; n=13 for both; see Table S3 for raw values.

G) Summary data of V_{50} values measured in WT, CB1RKO and CB1RKO+WIN.

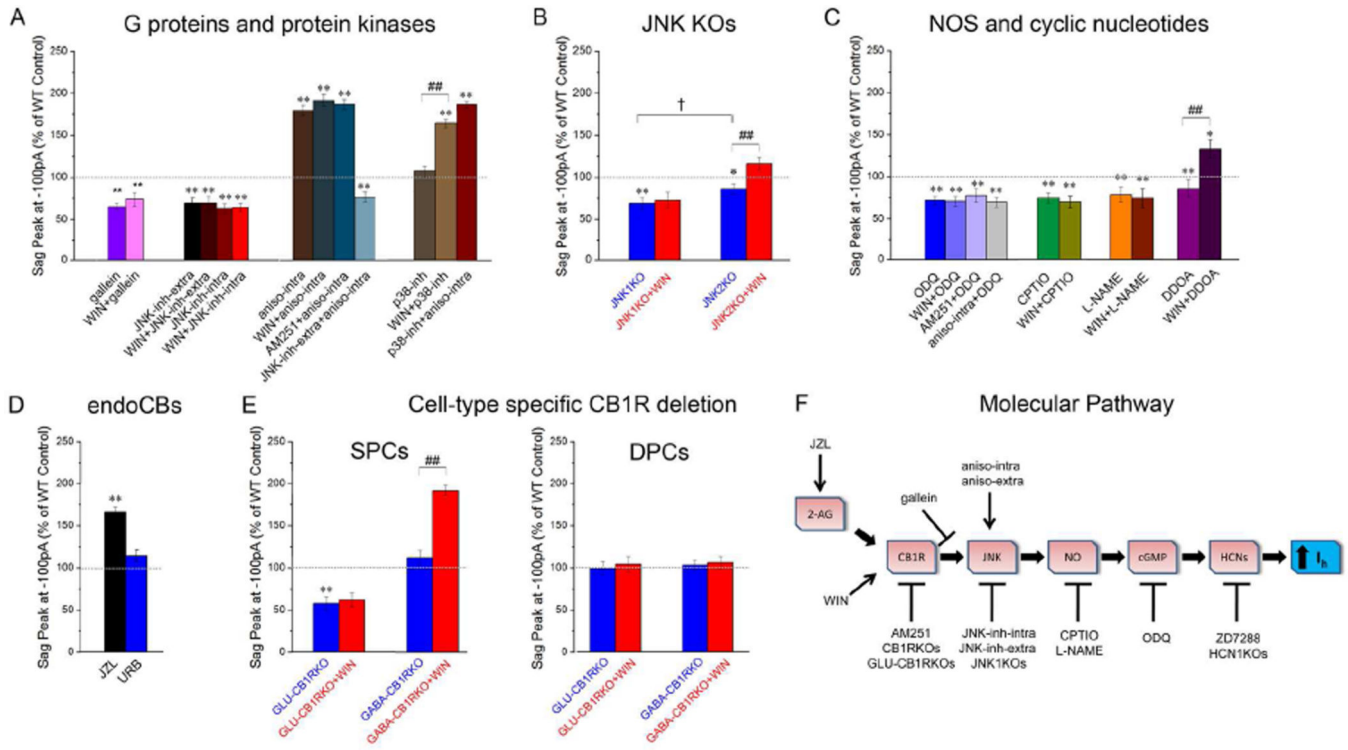

Figure 3. Molecular pathway underlying CB1R control of I_h

A–E) Peak sag amplitudes recorded at −100 pA are shown; stimulation protocol as in Fig. 1A. The effect on sag amplitude was similar for all current injections between −400 and −100 pA, see Table S1 (SPCs) and Table S2 (DPCs).

A) Participation of G proteins and protein kinases in SPCs (n: gallein: 12; WIN+gallein: 12; JNK-inh extra: 13; WIN+JNK-inh-extra: 13; JNK-inh-intra: 13; WIN+JNK-inh-intra: 13; aniso-intra: 14; WIN+aniso-intra: 14; AM251+aniso-intra: 15; JNK-inh-extra+aniso-intra: 11; p38-inh: 14; WIN+p38-inh: 14; p38-inh+aniso-intra: 12).

B) JNK1KO or JNK2KO SPCs, before (blue) and 4 min after WIN application (red) (n: JNK1KO: 13; JNK1KO+WIN: 13; JNK2KO: 11; JNK2KO+WIN: 11).

C) Participation of NOS and cGMP (n: ODQ: 15; WIN+ODQ: 15; AM251+ODQ: 14; aniso-intra+ODQ: 15; CPTIO: 6; WIN+CPTIO: 5; L-NAME: 5; WIN+ L-NAME: 6; DDOA: 5; WIN+DDOA: 5).

D) Participation of 2-AG but not anandamide, recordings from SPCs (n: JZL: 12; URB: 13).

E) Recordings from GLU-CB1RKO or GABA-CB1RKO, before (blue) and 4 min after WIN application in SPCs (red) (n: WT: 13; GLU-CB1RKO: 15; GABA-CB1RKO: 12) and DPCs (n=11–13 per group: WT: 13; GLU-CB1RKO: 12; GABA-CB1RKO: 11).

F) Summary diagram of the proposed CB1R-I_h molecular pathway, with the targets of the various pharmacological or genetic manipulations reported in panels A to E.

Statistical comparisons: *p<0.05, **p<0.01: experimental vs. WT control; ##: p<0.01 with versus without WIN; † p<0.05 JNK1KO vs. JNK2KO.

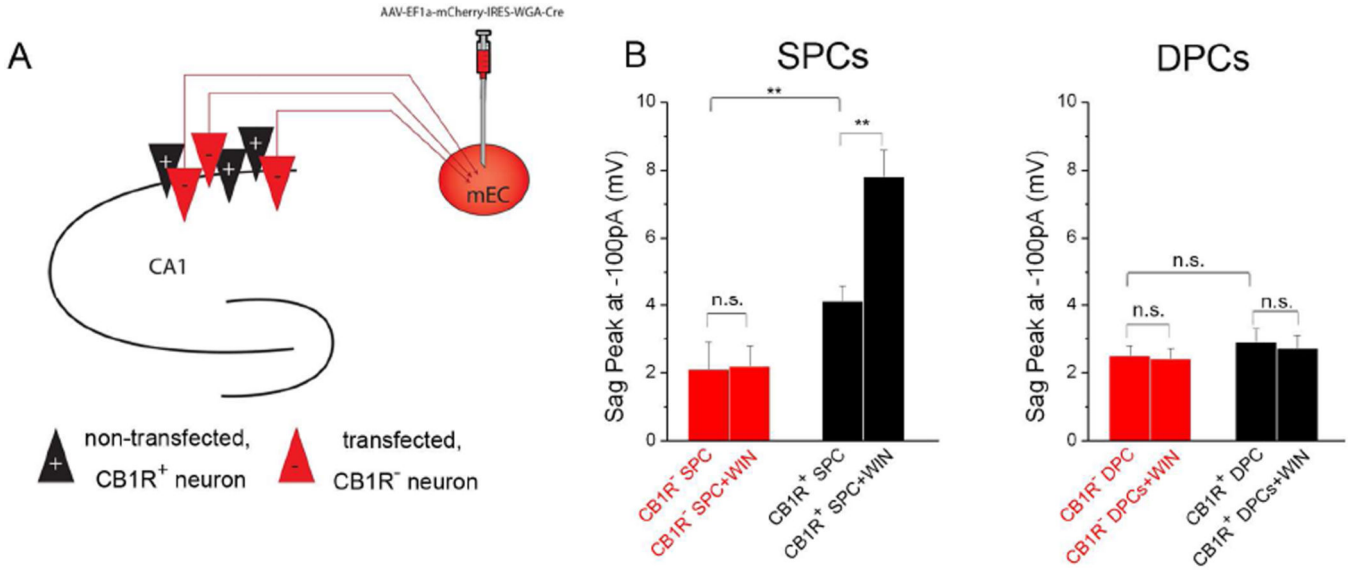

Figure 4. Postsynaptic CB1Rs modulate I_h in SPCs

A) Experimental paradigm. mEC: medial entorhinal cortex; Red triangle: cells expressing the viral vector, lacking CB1R ($CB1R^-$ cells); Black: uninfected, CB1R+ cells.

B) Peak sag amplitudes recorded at −100 pA in $CB1R^-$ and $CB1R^+$ SPCs (left) and DPCs (right) before and after WIN application (n: $CB1R^-$ SPCs: 10; $CB1R^-$ SPCs + WIN: 15; $CB1R^+$ SPCs: 13; $CB1R^+$ SPCs+WIN: 15; $CB1R^-$ DPCs: 11; $CB1R^-$ DPCs+WIN: 13; $CB1R^+$ DPCs: 14; $CB1R^+$ DPCs+WIN: 13). The effect on sag amplitude was similar for all current injections between −400 and −100 pA (Tables S1 and S2).

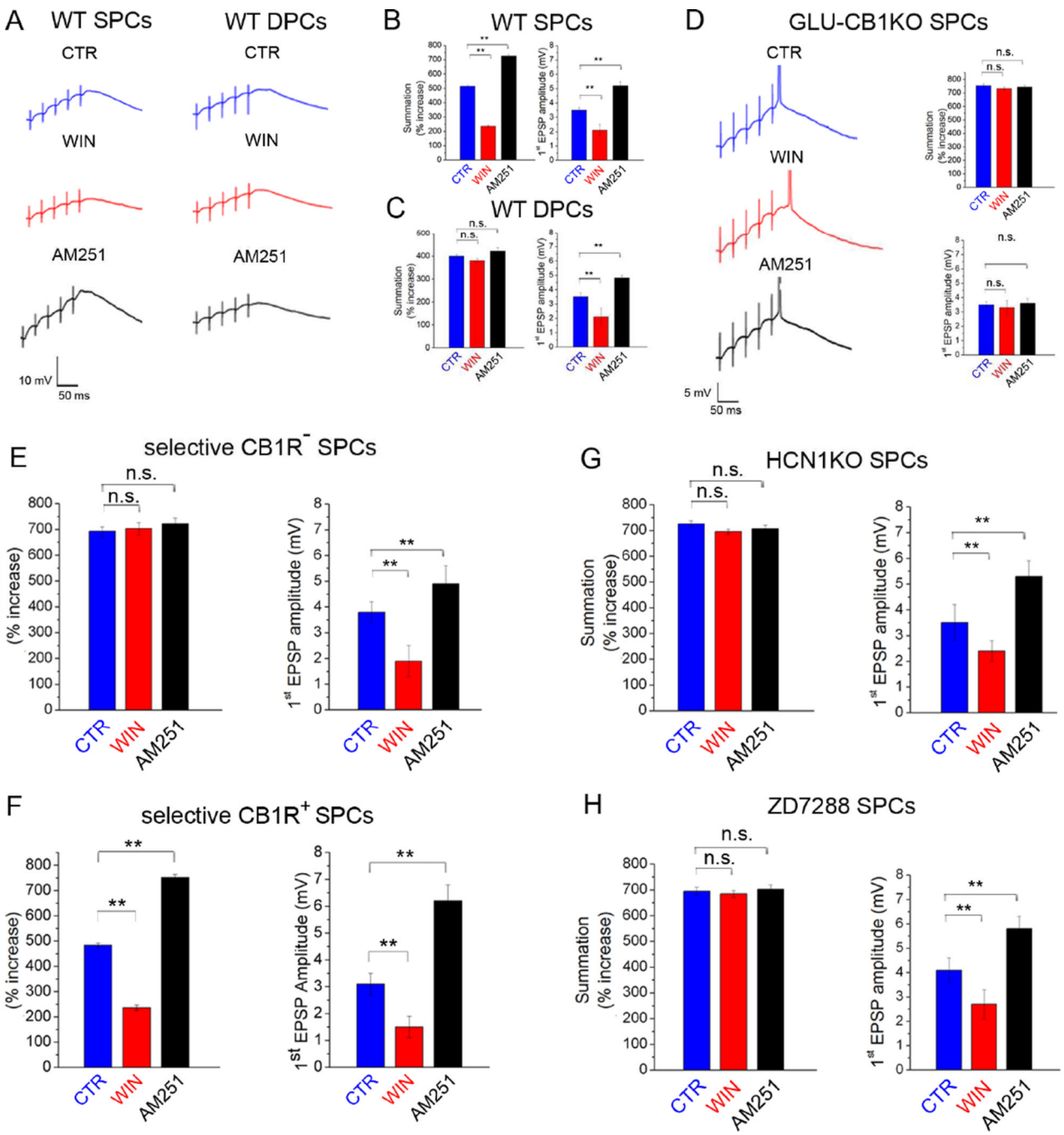

Figure 5. CB1Rs on glutamatergic cells modulate temporal summation of excitatory inputs in SPCs

A) Example traces (averages of ≥5) of EPSP trains evoked in SPCs and DPCs in WT mice in control conditions (CTR) and after bath application of WIN or AM251.

B,C) Summary data of EPSP summation and amplitude of first EPSPs in SPCs **(B)** and DPCs **(C)** in CTR and after WIN or AM251 application (n: CTR SPCs: 12; WIN SPCs: 12; AM251 SPCs: 15; CTR DPCs: 11; WIN DPCs: 14; AM251 DPCs: 11).

D) Traces of EPSP trains evoked in SPCs from GLU-CB1RKO mice in CTR and after WIN or AM251. Right: Summary data of EPSP summation and amplitude of first EPSPs (n: CTR: 15; WIN: 15; AM251: 14).

E, F) Summary data of EPSP summation and amplitude of first EPSPs in $CB1R^-$ SPCs **(E)** and in $CB1R^+$ **(F)** in CTR and after WIN or AM251 (n: CTR $CB1R^-$ 10; WIN $CB1R^-$: 10; AM251 $CB1R^-$: 11; CTR $CB1R^+$: 10; WIN $CB1R^+$: 10; AM251 + $CB1R^+$: 11).

G) Summary data of EPSP summation and amplitude of first EPSPs in SPCs from HCN1KOs in CTR and after WIN or AM251 (n: CTR: 9; WIN: 11; AM251: 11).

H) Summary data of EPSP summation and amplitude of first EPSPs in SPCs from ZD7288-treated slices in CTR and after WIN or AM251 application (n: CTR: 12; WIN: 14; AM251: 12).

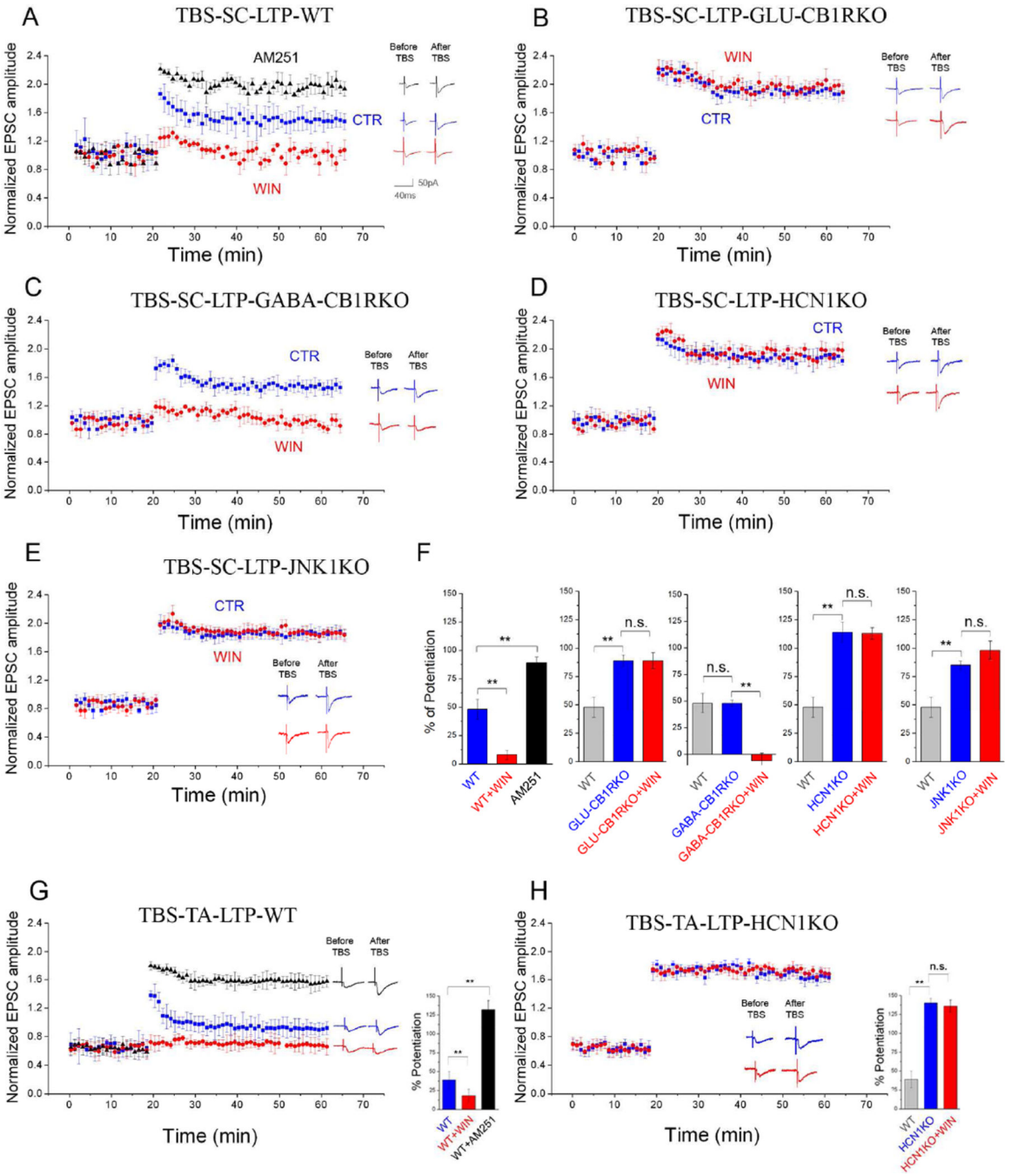

Figure 6. Effects of CB1R-mediated I_h modulation on LTP

A–E) Summary plots of the normalized EPSC amplitudes from SPCs before and after LTP induced by theta burst stimulation (TBS) at Schaffer collateral (SC) inputs (TBS-SC-LTP) from **(A)** WT (n=11), **(B)** GLU-CB1RKO (n=12), **(C)** GABA-CBARKO (n=14), **(D)** HCN1KO (n=13), and **(E)** JNK1KO (n=12), recorded in control perfusate (CTR, blue) or WIN (red) or AM251 (black). Examples traces were acquired 10min before and 60min after TBS.

F) Summary graphs of % potentiation of EPSC amplitudes 60min after TBS compared to 10min before.

G,H) Summary plots (as in A–E) induced by TBS at temporo-ammonic (TA) inputs (TBS-TA-LTP) in SPCs from WT **(G)** and HCN1KO **(H)** mice. Right: Bar graphs of % potentiation of EPSCs. **G)** Responses in CTR, WIN or AM251 (n: CTR: 11; WIN: 15; AM251: 10). **H)** Responses in CTR or WIN (n: CTR: 10; WIN: 13).

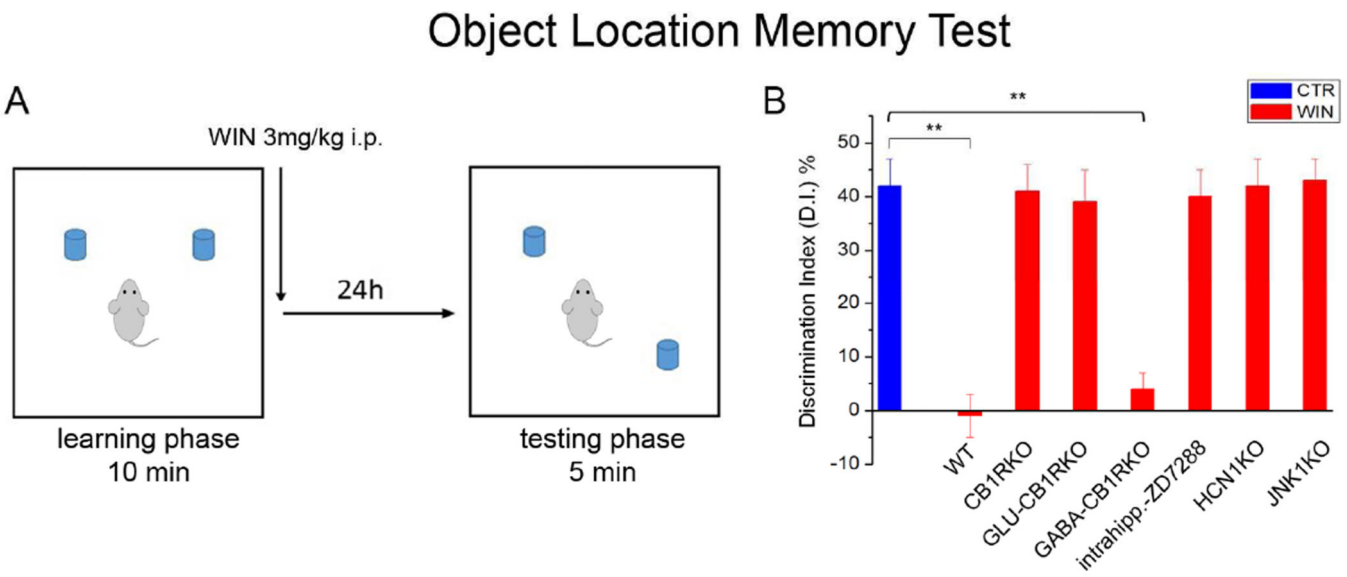

Figure 7. Effects of CB1R-mediated I_h modulation on spatial memory formation

A) Schematic representation of the object location memory task (OLM).

B) Bar graphs showing the discrimination index (DI), used to evaluate spatial memory formation, in vehicle-treated control animals (blue) and in WIN-treated WT, CB1RKO, GLU-CB1RKO, GABA-CB1RKO, HCN1KO and JNK1KO mice (red); vehicle-treated littermate controls showed statistically similar DI values, therefore, they were pooled together (n: Control: 72; WT: 16; CB1RKO: 18; GLUCB1RKO: 16; GABA-CB1RKO: 15; HCN1KO: 17; JNK1KO: 18).